coatings

MDPI

Article

One-Step Deposition of Polyester/TiO_2 Coatings by Atmospheric Pressure Plasma Jet on Wood Surfaces for UV and Moisture Protection

Ghiath Jnido *, Gisela Ohms and Wolfgang Viöl

Laboratory of Laser and Plasma Technologies, University of Applied Sciences and Arts, Von-Ossietzky-Str. 99, 37085 Göttingen, Germany; gisela.ohms@hawk.de (G.O.); wolfgang.vioel@hawk.de (W.V.)

* Correspondence: ghiath.jnido2@hawk.de

Received: 27 January 2020; Accepted: 17 February 2020; Published: 19 February 2020

Abstract: In this work, polyester/TiO_2 coatings on wood surfaces were prepared in one step via two deposition methods by using an atmospheric pressure plasma jet technique with the aim to further enhance the stabilization of the wood surfaces against UV-radiation and moisture. The first method, based on the combination of plasma spray powder (PSP) coating and liquid precursor plasma spraying (LPPS) coating techniques, used polyester powder and titanium tetraisopropoxide (TTIP) liquid precursor as feedstock. In the second method, the polyester/TiO_2 coatings were prepared by using a mixed powder of polyester micro-particles and TiO_2 nano-particles as feedstock and applied via plasma spray powder coating technique. The surface topology and morphology of the wood samples were observed by scanning electron microscopy (SEM). The SEM results showed the presence of a rough structure after coating with polyester/TiO_2. The surface chemical compositions of the samples were characterized by X-ray photoelectron spectroscopy and by Fourier transform infrared spectroscopy. The wetting behaviour of the coated wood surfaces was studied by measuring the water contact angle. After coating a hydrophilic wood surface with polyester/TiO_2 prepared via (PSP + LPPS), it showed excellent water repellency; the wood surfaces were transformed from hydrophilic to superhydrophobic, while the polyester/TiO_2 coating prepared via (PSP) was hydrophilic. Protection against UV radiation-induced colour changes was determined by UV tests and photo-assisted analysis using the CIELab colour system. The abrasion test results indicated that the polyester-containing films had good abrasion resistance and good adhesion to the wood substrates.

Keywords: atmospheric pressure plasma; wood; titanium dioxide; polyester; UV protection; superhydrophobic coating; abrasion resistance

1. Introduction

When wood products are exposed to environmental conditions without any protection, they are generally influenced by several weathering factors that modify their natural durability (reducing their mechanical stability) and aesthetic appearance (discolouration). Such factors are, for example, ultraviolet (UV) radiation, rainwater, temperature changes, and abrasion by wind-blown particles. The discolouration of unprotected wood surfaces is caused mainly by UV radiation and is a serious aesthetic problem for many outdoor applications such as terraces, garden constructions and furniture, facades, and balconies [1,2]. In order to keep the wood materials in optimal condition as long as possible, it is necessary to cover the wood surfaces with suitable protective coatings.

In recent years, the development of new inorganic/organic composites with unique properties has attracted great interest due to the enhanced properties of the composites compared to their pure components [3–6]. These composite materials combine the advantages of the inorganic

material (e.g., high refractivity, high mechanical and thermal stability) and the organic polymer (e.g., flexibility, durability, processability, and easy fabrication). These high-performance or high-functional materials have a wide range of potential uses in many innovative industrial applications [7]. Indeed, organic/inorganic composite materials consisting of titanium dioxide (TiO_2) have attracted much interest because adding titanium dioxide into polymers enhances the properties of polymers, leading to applications in several scientific and technological areas, such as anti-corrosion [8], anti-bactericidal [9–11], UV protection and photocatalysis [12,13], biotechnology, and the biomedical sector [14,15].

Titanium dioxide as coating material displays a number of fortunate properties. It is biologically and chemically inert, and photo- and thermally stable. Moreover, it possesses photocatalytic properties and is an inexpensive material of low toxicity [16,17]. It occurs in nature in three different crystalline structures, known as rutile (tetragonal), anatase (tetragonal) and brookite (orthorhombic).

Especially, rutile and anatase are frequently used materials in industrial applications. Depending on their crystal structures, the properties of the various crystal phases may vary. Thus, anatase is photocatalytically more active than the rutile. This is explained by the larger band gap of anatase when compared to the rutile phase (rutile: ~3.0 eV; anatase: ~3.2 eV) [17,18].

Recently, atmospheric plasma deposition techniques have been widely used in the production of hybrid materials [19,20]. Atmospheric plasma deposition can be used to prepare thin layers of material on a wide number of substrates. This may provide new functional properties for numerous applications in a cost-efficient way [21]. Moreover, the process produces only small amounts of side products and waste materials and enables flexible and fast processing. The application of atmospheric plasma at low temperatures allows to deposit films on organic, plastic and biological substrates [22,23]. Different variants of atmospheric plasma deposition techniques are used to deposit the coatings. One example is the liquid precursor plasma spraying (LPPS) deposition technique, in which the starting materials are liquid precursors; another method is the plasma spray powder (PSP) coating technique, in which powders are used as feedstock. A method consisting of hybrid processing using powders and liquid precursors by simultaneous feeding in plasma is used for developing composite coatings [24–26].

We have previously reported on the deposition of TiO_2 coatings from TTIP on wood surfaces deposited by using an atmospheric plasma jet system via the liquid precursor plasma spraying (LPPS) coating technique [27]. These TiO_2 coatings showed stability against ultraviolet light and good moisture resistance but a lower adhesion to the wood substrates. Köhler et al. [28,29] reported on the deposition of polyester coatings on wood surfaces deposited by using an atmospheric plasma jet via plasma spray powder (PSP) coating technique. The adhesion of the polyester coatings was good with an average pull-off strength of > 1 MPa. In the present work, a combination between the advantages of the TiO_2 coatings (UV-protection and moisture protection) and the polyester coatings (good adhesion and moisture protection) was produced. These polyester/TiO_2 composite coatings are expected to provide the best properties and functions of both materials (polyester and TiO_2), such as high mechanical properties (good adhesion to wood surfaces), high UV resistance, and high stability and water repellency, which are not achieved by either material alone.

2. Materials and Methods

The polyester/TiO_2 films were obtained applying an atmospheric pressure plasma jet system (APPJ) system (Reinhausen Plasma GmbH, Regensburg, Germany), which has already been described by several authors [28,30,31]. The schematic setup of the experiment is visualized in Figure 1. It includes an atomizing nozzle attached to the plasma gun to spray the solution precursor. A powder feeder introduces the powder into the plasma jet. The working gas was compressed air, fed to the plasma torch with a fixed flow rate of 60 L/min during the deposition. The plasma was generated between two tubular electrodes applying an ignition voltage of ca. 15 kV, whereas the effective voltage was 2–3 kV. The pulses last about 5–10 µs and were repeated using a frequency of 50 kHz. The electrical power in the experiments was 2 kW. The nozzle was adjusted 24 mm above the substrate applying a

plasma of a diameter of about 4 mm. To obtain the coatings, the samples were moved by a xy-linear stage with scan speed fixed at 40 mm/s. The spraying system AGF 10.0 (Palas GmbH, Karlsruhe, Germany) was used to introduce a solution precursor as spray into the plasma jet.

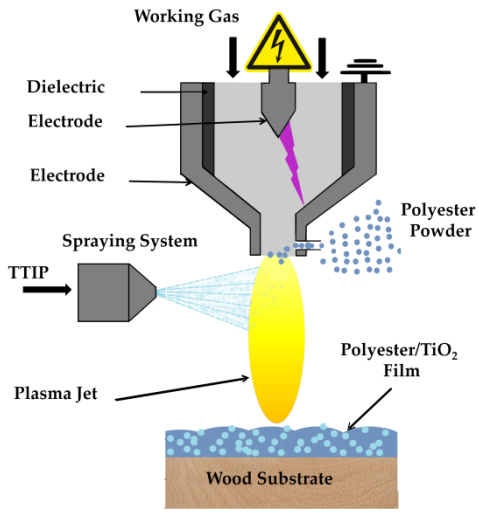

Figure 1. Scheme of the experimental setup for the deposition of polyester/TiO_2 films on wood substrate.

Titanium tetraisopropoxide (TTIP, $Ti(OC_3H_7)_4$, 97%, Sigma Aldrich, Saint Louis, MO, USA) was used as the metalorganic precursor to obtain TiO_2 films. The liquid precursor TTIP was nebulized with a cyclone (cut-off diameter of 10 µm) and sprayed into the plasma jet at the nearest position to the outlet of the plasma nozzle. Nitrogen was used as a carrier gas to spray the precursor.

The powder disperser RBG 2000 (Palas GmbH, Karlsruhe, Germany) was applied as the powder feeder to introduce the powder into the plasma jet. A polyester powder (D_{50} = 45 µm), Interpon 610 MZ013GF (Akzo Nobel Powder Coatings GmbH, Arnsberg, Germany), based on an iso- and terephthalic acid (TPA) polyester mix with a density of 120 g/m^3, was used to generate polyester films. Here, to generate the particle aerosol, the powder was uniformly filled into a cylindrical feed stock reservoir and was moved towards a rotating dispersion brush by means of a piston at a constant speed, which defines the speed feed rate. The brush removed the powder from the reservoir. This powder was then dispersed from the rotating brush and carried by an air stream towards the plasma jet. As the carrier gas, compressed air with a pressure of 1.6×10^5 Pa was used in this study. The rotating speed of the brush was fixed at 1200 rpm. A reservoir with a cavity of 28 mm in diameter was used. Table 1 shows the coating parameters.

Table 1. Deposition parameters.

Sample	Deposition Technique	Working Distance (mm)	Powder Feed Speed (mm/h)	TTIP Carrier Gas N_2 (L/min)
Polyester/TiO_2 thick film	PSP + LPPS	24	150	14
Polyester/TiO_2 thin film	PSP + LPPS	24	50	17
Polyester/TiO_2 film	PSP	20	50	-
Polyester thick film	PSP	24	150	-
Polyester thin film	PSP	24	50	-
TiO_2 film	LPPS	24	-	14

In the second deposition method, TiO_2 nano-powder of 21 nm primary particle size (TEM), ≥ 99.5% trace metals basis (Sigma Aldrich, Saint Louis, MO, USA), was mixed with the polyester powder (30% TiO_2, 70% polyester) to obtain polyester/TiO_2 coatings via the plasma spray powder (PSP) coating technique. Here, the distance between the plasma nozzle and substrate was fixed at 20 mm, and the powder feed speed was set at 50 mm/h.

Samples of defect-free European beech (*Fagus sylvatica* L.) and Scots pine (*Pinus sylvestris* L.) sapwood were prepared with sample sizes of 76 mm × 26 mm × 4 mm (length × width × height). Before the plasma treatment, all samples were allowed to establish a moisture equilibrium by storing the samples at 20 °C and a relative humidity of 65% for 10 days.

In order to determine the thickness and chemical composition (FTIR) of the coatings, some glass samples were prepared in the same process.

The morphology of the polyester/TiO_2 films was examined by scanning electron microscopy (JEOL JSM-5600LV, Tokyo, Japan) at an accelerating voltage of 12 kV. All samples were sputter-coated with a thin gold film (20 nm) to avoid charging effects.

A 3D digital microscope VHX-6000 (Keyence GmbH, Neu-Isenburg, Germany) was used to measure the thickness of the coatings and to evaluate their surface roughness.

The control and the coated samples were investigated using a FTIR spectrometer (PerkinElmer Frontier spectrometer, Waltham, MA, USA). The samples were prepared using the KBr pellet technique. In addition, the samples were investigated by the attenuated total reflectance (ATR) method. For this, the FTIR spectrometer has been equipped with a special ATR set (Golden Gate Single Reflection Diamond ATR, Specac, Orpington, UK). All spectra were recorded between 4000 cm^{-1} and 400 cm^{-1} at a resolution of 4 cm^{-1} and a number of 64 scans.

In order to identify the chemical composition of the polyester/TiO_2 films deposited on wood surfaces, we used X-ray photoelectron spectroscopy using a PHI 5000 Versa Probe II (ULVAC-PHI, Chigasaki, Japan). The instrument uses a monochromatic Al K_α source with a photon energy of 1486.6 eV to irradiate a spot of 200 μm in diameter. Survey spectra were obtained at a pass energy of 187.85 eV, and the high-resolution spectra were scanned at a pass energy of 23.5 eV with a step size of 0.1 eV. The resulting spectra were analyzed using the software MultiPak (ULVAC-PHI, Chigasaki, Japan).

To evaluate the efficiency of UV protection, the polyester/TiO_2-coated samples were exposed to UVA light (λ = 365 nm) at room temperature using a UV lamp (Herolab GmbH, Wiesloch, Germany) with a power input of 8 W. The light intensity was 950 μW/cm^2. The wood samples were exposed to UV light for a total of 200 h and their colour change was monitored in intervals of 10 h. The experiment was performed using three similar samples for each coating composite. The colour values (CIELAB L^*, a^*, b^*, parameters) of the samples were determined in the given intervals and the average values were calculated. A digital camera EOS 600D (Canon Inc., Tokyo, Japan) was used for colour measurement. The colour measurement method was described in our previous paper [27].

The CIELab system used in this study is characterized by three parameters: L^*, a^*, and b^*. The L^* coordinate represents the lightness and varies from 0 (black) to 100 (white); a^* and b^* are the chromatic indices of colour; $+a^*$ is the red direction; $-a^*$ is green; $+b^*$ is yellow; and $-b^*$ is blue. The L^*, a^*, and b^* colour coordinates of each examined sample before and after UV irradiation were used to calculate the total colour change ΔE^* according to the following equation:

$$\Delta E^* = (\Delta L^{*2} + \Delta a^{*2} + \Delta b^{*2})^{1/2} \quad (1)$$

where Δ means the difference between the indicated final and initial parameters after UV irradiation [32]. A low ΔE^* value corresponds to a small colour change and indicates that the samples are less sensitive to UV radiation [33].

The water contact angle (WCA) was measured to evaluate the wettability of the uncoated and coated wood samples using a Mobile Surface Analyzer-MSA (Krüss GmbH, Hamburg, Germany). The contact angle measurements were performed with distilled water at room temperature. Water drops with volumes of 1 μL were applied. As there is a change of contact angles with time, all values were recorded after a constant elapsed time of 10 s. For each of the samples, five separate measurements were carried out, and the average value of the measurements was calculated.

3. Results and Discussion

3.1. Characterization of Coatings on Wood by Scanning Electron Microscopy (SEM)

The microstructure and morphology of the uncoated wood and coated wood surfaces were examined by Scanning electron microscopy. Here, only the SEM-images of the beech samples are shown, because the surface morphologies of the pine samples were similar to the surface morphologies of the beech samples. Figures 2 and 3 show the SEM-images of the beech wood samples observed with a magnification of 100× and 2000×, respectively. The images at the lower magnification of 100× show the structural alterations to the beech wood sample after the coating, while the images at the higher magnifications of 2000× show clearly the microstructure and morphology of the coatings. Figure 2a shows that the native wood presents a smooth surface with several vessels on the surface. As can be seen in Figure 2b, the small TiO_2 particles, deposited from the TTIP precursor, cover the wood surface, but the microstructure of the wood surface is still visible. Figure 2c shows that the polyester film deposited at a speed feed rate of 150 mm/h has totally covered the wood surface and formed a smooth coating with some pores and small protrusions at the surface, but the microstructure of wood cannot be seen. The same microstructure was recorded for the polyester film deposited at a speed feed rate of 50 mm/h. Figure 2d shows that the polyester/TiO_2 composite coating deposited at a speed feed rate of 150 mm/h has totally covered the wood surface and formed a rough and porous layer. The wood structure was still clearly visible for the wood surface coated with polyester/TiO_2 composite deposited at a speed feed rate of 50 mm/h, as is shown in Figure 2e. Figure 2f shows the surface morphology of the composite coating obtained at a powder feed speed of 50 mm/h via the (PSP) deposition technique. It can be seen that the wood surface became rough and totally covered with coating but some vessels on the surface are not completely filled with the particles. The polyester/TiO_2 composite coating, obtained via the (PSP) deposition technique, appeared to be relatively dense compared to the composite coatings from the other deposition technique.

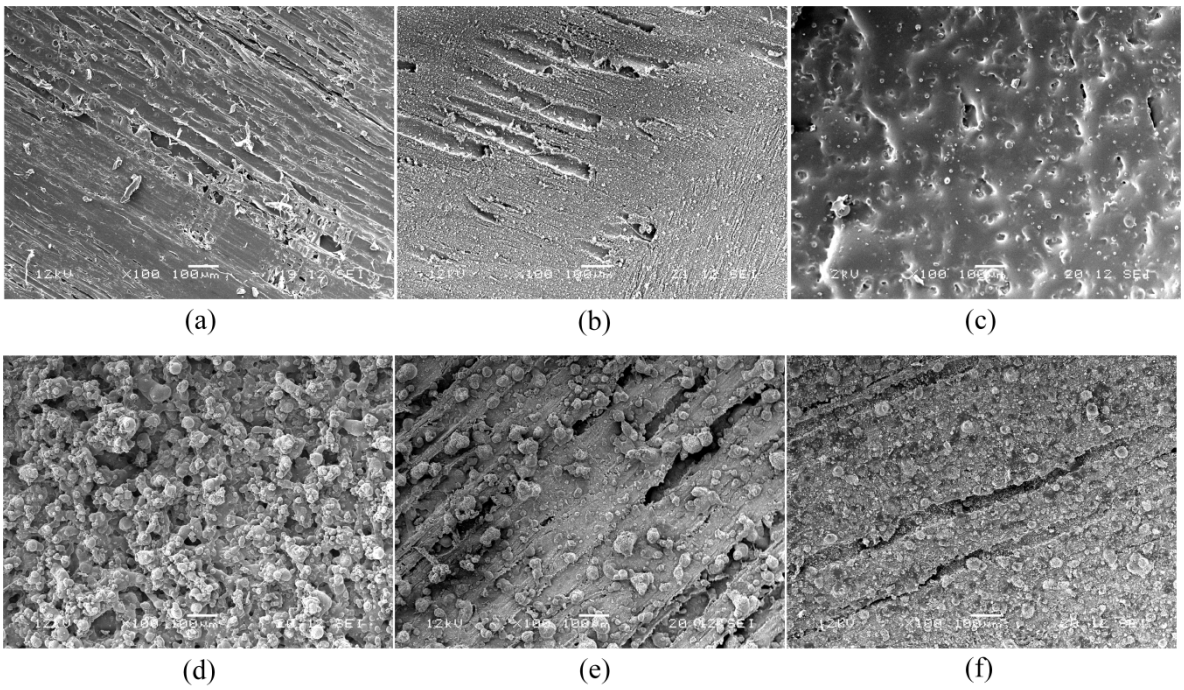

Figure 2. SEM-images with a magnification of 100× (scale bar 100 μm): (**a**) uncoated wood beech; (**b**) TiO_2 film; (**c**) polyester thick film; (**d**) polyester/TiO_2 thick film; (**e**) polyester/TiO_2 thin film; (**f**) polyester/TiO_2 film via (PSP).

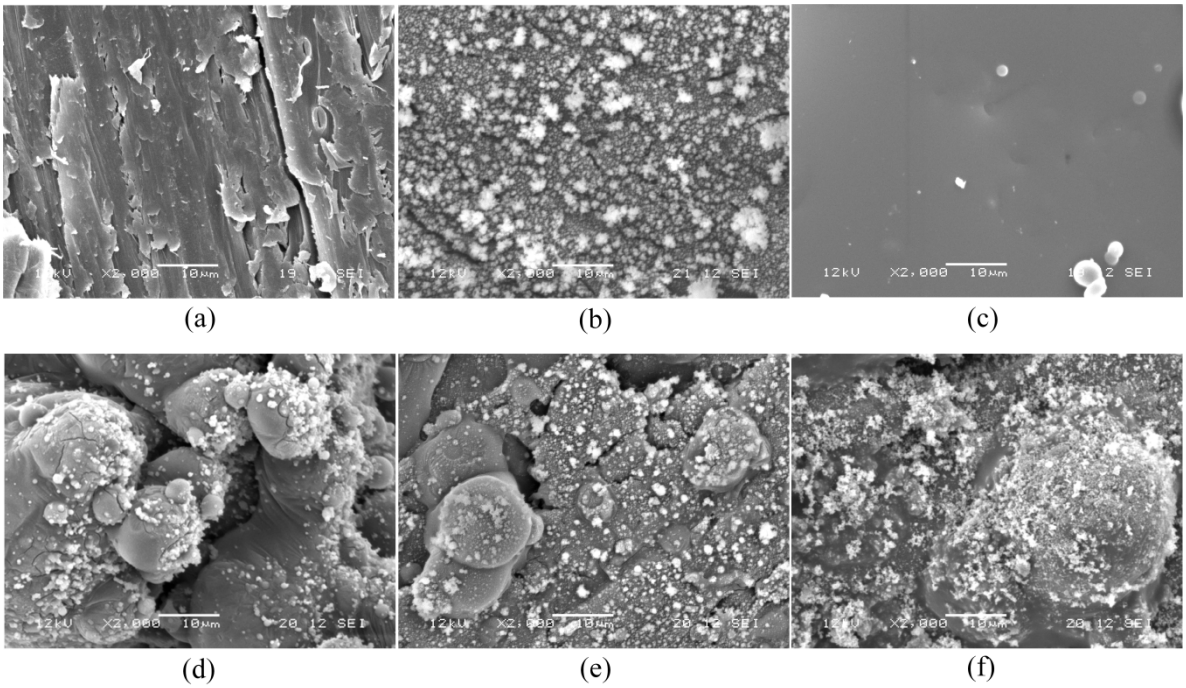

Figure 3. SEM-images with a magnification of 2000× (scale bar 10 μm): (**a**) uncoated wood beech; (**b**) TiO_2 film; (**c**) polyester thick film; (**d**) polyester/TiO_2 thick film; (**e**) polyester/TiO_2 thin film; (**f**) polyester/TiO_2 film via (PSP).

SEM-images of the samples at the magnifications of 2000× give better information about the microstructure of the coatings. Figure 3a shows that the natural wood sample has a smooth surface. The deposition of TiO_2 from TTIP (Figure 3b) results in the growth of small TiO_2 globules with some areas agglomerated on the surface of wood. The dimension of agglomerates was 5–8 μm. The surface of the wood with only polyester coating (Figure 3c) is very smooth with a small number of unmelted particles located on the surface. From Figure 3d,e, it can be seen that the polyester/TiO_2 composite coatings were porous, consisting of unmelted and semi-melted polyester spherical particles with size variations from 1 μm to more than 12 μm. Furthermore, the globules of TiO_2 are linked to the polyester structure. It could be noticed that the globules of TiO_2 are similar to the globules of TiO_2 coatings deposited on wood surfaces without polyester. The dimension of TiO_2-agglomerates was ~3 μm. The polyester/TiO_2 composite coating, obtained via the (PSP) technique (Figure 3f), appeared to be porous, consisting of small melted particles, as well as semi-melted spherical particles. The TiO_2 nanoparticles are present as small globules and linked to the polyester structure.

The thickness of the coatings was measured by 3D digital microscope. For this purpose, samples of glass were masked on one edge before the coating process. The average thicknesses of the coatings are given in Table 2.

Table 2. Average thicknesses of the coatings.

Sample	Deposition Technique	Powder Feed Rates (mm/h)	Thickness (μm)
Polyester thick film	PSP	150	114
Polyester/TiO_2 thick film	PSP + LPPS	150	112
Polyester thin film	PSP	50	36
Polyester/TiO_2 thin film	PSP + LPPS	50	22
Polyester/TiO_2 film	PSP	50	14
TiO_2 film	LPPS	-	0.35

3.2. Characterization of Coatings by Fourier Transform Infrared (FTIR) Spectroscopy

The chemical composition of the coated and uncoated wood surfaces was investigated with the FTIR spectroscopy (see Figure 4). Figure 4a shows the FTIR spectra of the coated wood samples examined by ATR. The FTIR–ATR spectrum of the TiO_2-coated wood differs slightly from that of the untreated sample. The strengthening of the band at 800–400 cm^{-1} is the most significant deviation. The band at 800–400 cm^{-1} can be attributed to a stretch vibration of the Ti–O–Ti [34,35], of the TiO_2 films grown directly on the surface of the wood samples. There is a considerable difference between the FTIR–ATR spectra of the polyester- and the polyester/TiO_2-coated wood in comparison to those of the uncoated wood. The disappearance of wood peaks indicates that the polyester and polyester/ TiO_2 films had covered the wood surfaces with thick layers. In the polyester and polyester/TiO_2 films spectra, the peaks at 2970 and 2893 cm^{-1} are assigned to the asymmetric and symmetric stretching vibrations of $–CH_2$, respectively. The very intense absorption peak observed at 1724 cm^{-1} is caused by the stretching vibration of ester carbonyl C=O. The peaks found at 1609 and 1508 cm^{-1} are assigned to the C=C stretching vibrations of the aromatic ring. The peak at 1477 cm^{-1} is due to the torsional vibrations of CH_2 groups, and the strong peaks at 1241 cm^{-1} and 1099 cm^{-1} are assigned to the asymmetric and symmetric valence vibration of C–O–C bonds, respectively [36,37].

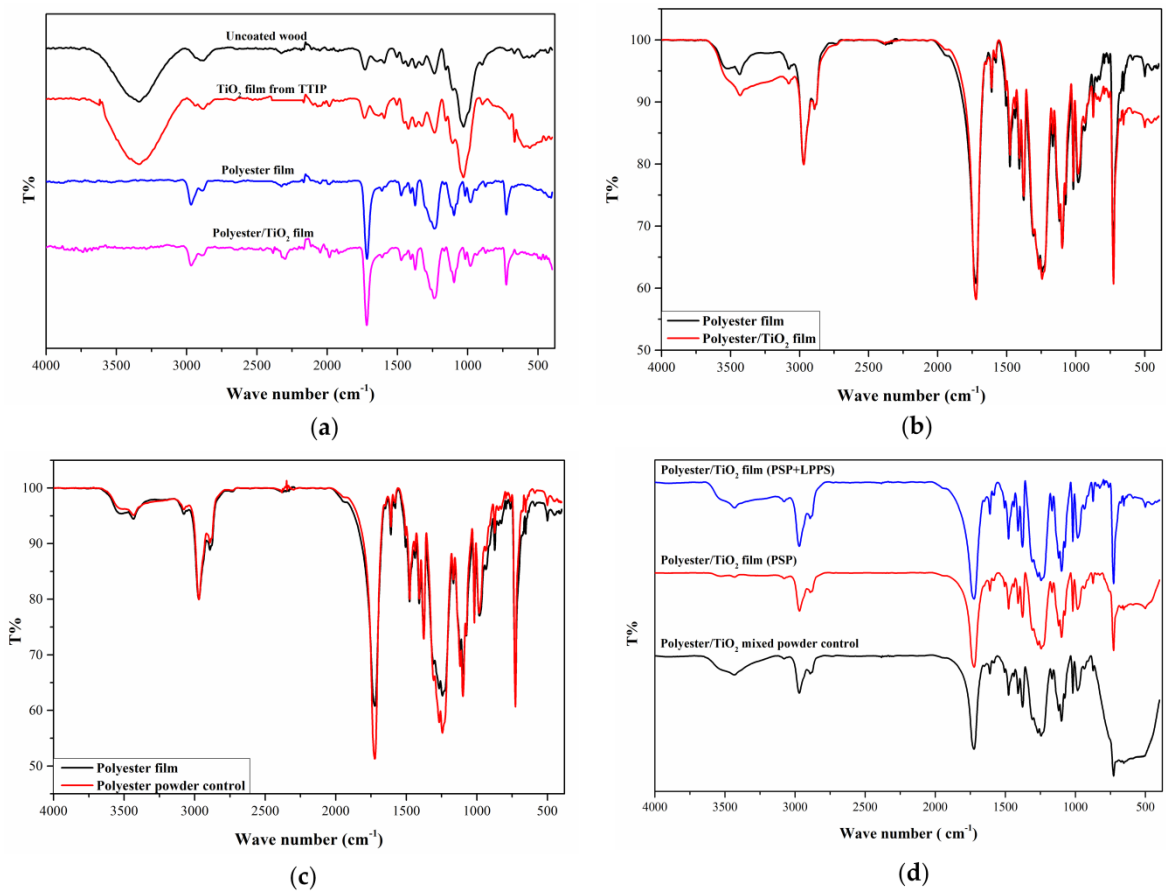

Figure 4. (**a**) FTIR–ATR spectra for uncoated wood and coated wood; (**b**) FTIR spectra for polyester and polyester/TiO_2 films; (**c**) FTIR spectra for polyester powder reference and polyester film; (**d**) FTIR spectra for polyester/TiO_2 powder reference and polyester/TiO_2 films.

FTIR analysis was performed on polyester/TiO_2 powders using the KBr Pellet technique. For this purpose, some coatings were taken from the substrates to prepare powder samples. Figure 4b visualizes the differences between the KBr-FTIR spectrum of the polyester/TiO_2-coated wood and the polyester-coated wood, respectively. The obvious differences were the strengthening of the bands

at 800–400 cm^{-1} for the polyester/TiO_2-coated sample, indicating the incorporation of TiO_2 particles inside the polyester matrix. From Figure 4c, it is clear that there are no significant differences in the FTIR spectra of the polyester powder reference and polyester after deposition using atmospheric pressure plasma. Figure 4d displays the KBr-FTIR spectra of the polyester/TiO_2 as reference and polyester/TiO_2 films obtained from both deposition methods. The spectra of the three samples showed approximately similar peaks but differences in two regions, between 3500–3000 cm^{-1} and below 750 cm^{-1}. From the spectrum of the film obtained via the (PSP) method, it can be seen that the –OH peak almost disappeared, while the Ti–O peak is clearly visible. In the spectrum of the film obtained via the combination of the (PSP) and (LPPS) coating methods, the intensity of absorption bands corresponding to Ti–O is very small compared with the (PSP) method. By using TTIP, additional hydroxyl groups OH were produced, e.g., $TiO(OH)_2$. The absence of hydroxyl groups in the spectrum of the polyester/TiO_2 film obtained via the (PSP) method suggests that the hydroxyl groups OH, which were present in the spectra of the starting material polyester /titanium oxide mixture, were lost; they could have dried during the coating by the plasma jet.

3.3. Characterization of Coatings by X-ray Photoelectron Spectroscopy (XPS)

To investigate further the elemental composition and surface chemical state of the polyester and polyester/TiO_2-coated wood surfaces, X-Ray photoelectron spectroscopy (XPS) measurements were carried out. The XPS results are presented in Figure 5. Figure 5a shows the XPS survey spectra of uncoated wood, polyester film and of the thick polyester /TiO_2 film obtained via the combination of the (PSP) and (LPPS) coating methods. On the survey spectrum of uncoated wood, the presence of oxygen and carbon could be identified, whereas the survey spectrum of polyester film detects oxygen, carbon and a small additional peak for nitrogen. For the polyester/TiO_2 film, the titanium peak is recorded in addition to the oxygen, carbon and nitrogen peaks. The results of the elemental composition calculated from the measured XPS spectrum of the different coatings on wood substrates are summarized in Table 3.

Table 3. Surface composition of different coatings observed in the XPS spectra.

Sample	Surface Composition (at.%)			
	C	O	Ti	N
Uncoated wood	69.2	30.8	-	-
Polyester thick film	62.60	33.98	-	3.42
Polyester/TiO_2 thick film	49.85	39.96	7.26	2.93
Polyester/TiO_2 thin film	48.45	41.78	9.53	0.24
Polyester/TiO_2 film via (PSP)	48.69	40.53	7.57	3.21

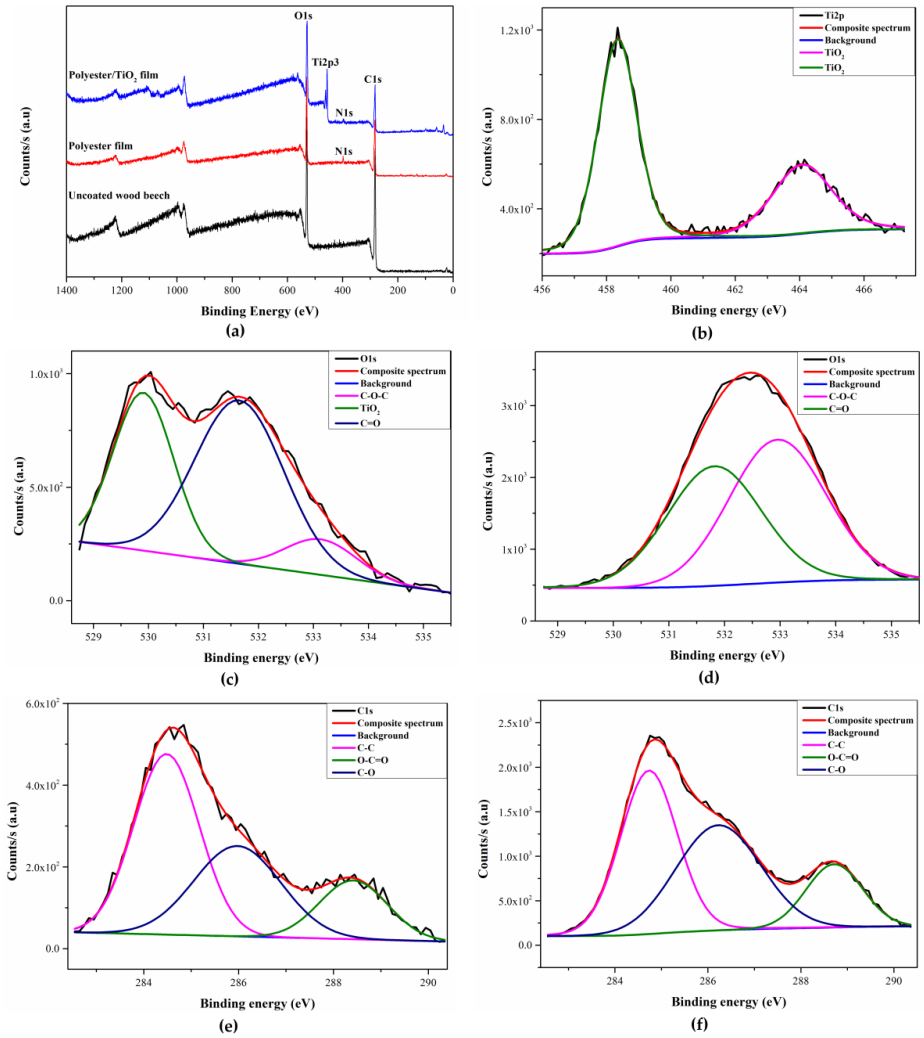

Figure 5. XPS survey spectra and high resolution XPS spectra of the uncoated wood, polyester-coated wood and polyester/TiO_2-coated wood; (**a**) survey spectra; (**b**) high-resolution XPS spectra of Ti 2p; (**c**) O 1s for polyester/TiO_2 film; (**d**) O 1s for polyester film; (**e**) C 1s for polyester/TiO_2 film; (**f**) C 1s for polyester film.

For more detailed information on the binding energies of the elements on the coated surfaces, high-resolution XPS spectra of the C 1*s*, O 1*s*, and Ti 2*p* regions were investigated. All spectra were analysed using the symmetrical Gaussian/Lorentzian fitting function. The binding energy values were corrected by calibration and adjusting the C 1*s* line to a value of 284.8 eV [38].

In Figure 5b, the Ti *2p* high resolved spectrum of the polyester/TiO_2 film is shown. This spectrum consists of a doublet peak. According to the Ti *2p* peak deconvolution, the intense peaks Ti $2p_{1/2}$ (464.07 eV) and Ti $2p_{3/2}$ (458.34 eV) are assigned to Ti^{4+} (TiO_2) [31]. Figure 5c visualizes the high-resolution spectrum of O 1s of the polyester/TiO_2 film. The deconvolution of the O *1s* peak leads to three peaks at 529.81, 531.61 and 533.34 eV, corresponding to Ti–O (TiO_2), C=O and C–O, respectively [31]. From the deconvolution of the high-resolution spectrum of O 1s, two peaks at 531.75 and 532.96 eV were computed for the polyester film. These correspond to O=C–O (ester group) and C-O, respectively [28,31]. This is displayed in Figure 5d. The high-resolution spectra of C *1s* for the polyester film (Figure 5e) and polyester/TiO_2 film (Figure 5f) are similar. The C *1s* peak can be deconvoluted into three peaks located at 284.73 eV, 286.22 eV and 288.71 eV corresponding to C–C or C–H, C–O and O=C–O (ester group), respectively [28,31,38].

3.4. Ultraviolet (UV) Protection

The UV-protection efficiency of the polyester/TiO_2 coatings on the wood samples was studied by monitoring the colour change over a period of time. The experiment was performed using three samples for each coating composite. The colour values of the samples were measured every 10 h, and the average values were calculated. The results of the colour measurements of the coated and control wood samples as a function of the UV irradiation time are summarized in Table 4. The evolution of the total colour change ΔE^* of the polyester/TiO_2 coatings with increasing UV irradiation time is shown in Figure 6. It is obvious that the uncoated wood samples underwent the strongest discolouration after 200 h. Here, the discolouration ΔE^* reached the values of 9.49 for beech wood and 13.36 for pine wood. In contrast, the wood samples coated with the polyester/TiO_2 film showed only a minor discolouration, which remained stable throughout the whole UV irradiation time.

Table 4. Differences in colour measurements before and after 200 h exposure to UVA radiation.

Species	Sample	ΔL^*	Δa^*	Δb^*	ΔE^*
Beech	Control	−3.36	2.13	8.15	9.49
	Polyester/TiO_2 thick film	−2.49	0.71	1.02	2.82
	Polyester/TiO_2 thin film	−2.57	1.96	1.81	3.76
	Polyester/TiO_2 film via (PSP)	−2.01	0.75	0.7	2.62
Pine	Control	−3.66	1.76	12.83	13.36
	Polyester/TiO_2 thick film	−0.48	−0.24	1.76	1.85
	Polyester/TiO_2 thin film	−2.72	1.22	4.66	7.76
	Polyester/TiO_2 film via (PSP)	−1.45	1.10	3.90	3.86

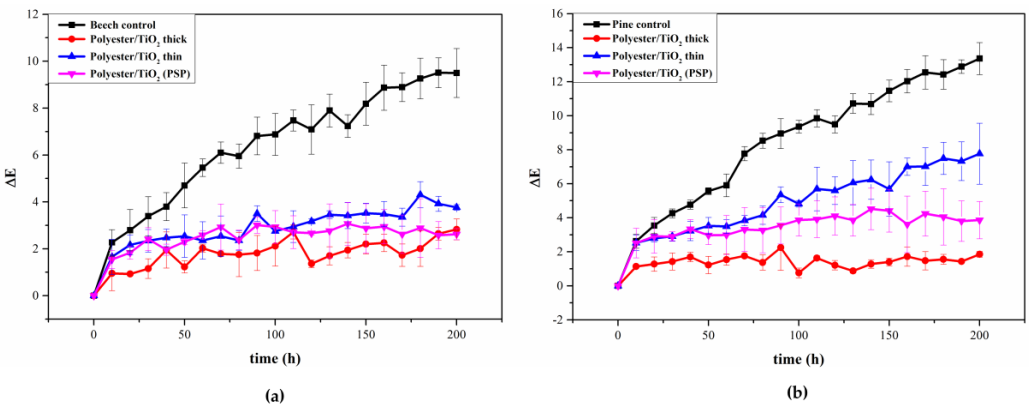

Figure 6. Change of total colour ΔE^* of coated and uncoated wood samples depending upon the time of irradiation of (**a**) beech and (**b**) pine.

From Table 4, the negative values of lightness (ΔL^*) indicate that all samples became darker after 200 h exposure to UVA radiation. Here, the brightness loss ΔL^* was about −3.5 for both pine and beech wood without UV-protecting coating. By comparison, the brightness change ΔL^* of the beech samples coated with the polyester/TiO_2 films were −2.49, −2.57 and −2.01 for thick film, thin film and the film obtained via the (PSP), respectively. In pine wood, the brightness change ΔL^* of the samples coated with the polyester/TiO_2 films was −0.48, −2.72 and −1.45 for thick film, thin film and the film obtained via the (PSP), respectively. The Δb^* values of the samples without UV-protective coatings reached 8.15 for beech wood and 12.83 for pine wood after 200 h irradiation. However, the Δb^* change of the polyester/TiO_2-coated wood samples was considerably smaller than that of the uncoated wood samples. The change in the Δb^* value indicated that UV irradiation forces the wood surface of the uncoated and polyester/TiO_2-coated samples to become yellowish. The colour is darker for the uncoated and only light yellow for the polyester/TiO_2-coated samples. The Δb^* value of the coated pine wood samples was slightly bigger than that of the coated beech samples, meaning that the colour of the pine wood

samples turned darker yellowish than that of beech wood samples. The Δa^* values of all uncoated wood and polyester/TiO_2-coated samples increased slightly after 200 h irradiation. The samples turned to a reddish colour after irradiation. This can be seen from the increase of the Δa^* values.

The photograph in Figure 7 shows the colour change of wood for the uncoated and polyester/TiO_2-coated samples after 50, 100, 150, and 200 h of exposure. Here, we can note that the colour change in the uncoated wood is clearly recognizable but the colour change in the polyester/TiO_2-coated wood is not immediately visible, indicating that the polyester/TiO_2-coated wood is more stable during 200 h of UV irradiation than uncoated wood. High colour stability could be reached if the wood surface had been coated with the thick polyester/TiO_2 films. No significant differences in colour measurements were observed between the deposition methods.

Figure 7. Visual appearance of coated and uncoated samples, before and after 50, 100, 150, and 200 h of UV- irradiation: (**a**) control beech wood; (**b**) control pine wood; (**c**) beech wood coated with polyester/TiO_2 thick film; (**d**) pine wood coated with polyester/TiO_2 thick film; (**e**) beech wood coated with polyester/TiO_2 film via (PSP); (**f**) pine wood coated with polyester/TiO_2 film via (PSP).

3.5. Abrasion Test

In order to evaluate the mechanical stability of the coatings, an abrasion test was carried out using a setup according to DIN ISO 9211-4 [39]. Here, the rubbing head of the abrasion tester was covered with cotton tissues. It was pressed to the surface of the coated samples with a force of (5 N ± 1 N) and moved back and forth linearly over the coated surface 2000 times (1000 cycles). Scanning electron microscope was used in order to evaluate the abrasion resistance of the coated samples. Figure 8 displays the surface morphologies of the coated wood before and after the abrasion test. Figure 8a,b show the SEM-images of the beech wood samples coated with thick and thin polyester coatings before and after the abrasion test, respectively. The surfaces of both polyester coatings show that the small pores became bigger, and the small unmelted particles were removed by the abrasion action. In addition, slight scratches in the direction of movement could be found. Figure 8c shows the SEM-images of the beech wood samples coated with thick polyester/TiO_2 coating before and after the abrasion test. The surface of the polyester/TiO_2 coatings changed from a rough surface into a smooth surface, and the spherical unmelted and semi-melted agglomerates were completely removed. Similar to the polyester coatings, slight scratches in the direction of movement could be found. Similar results were observed for the wood surfaces coated with thin polyester/TiO_2 coatings obtained via both deposition methods, as shown in Figure 8d,e. Figure 8f shows that the TiO_2 film on wood is completely removed after only 100 cycles. In Table 5, a remarkable decrease of the surface roughness average (*Sa*) of the surface for all samples after the abrasion action can be seen. These results indicate that the polyester-containing films had good abrasion resistance and adhesion to the wood substrates. However, at the end of the abrasion test, all the surfaces were slightly damaged. For the thickly coated surfaces, the amount of damages produced is, however, very small, as shown in Figure 9. For the thin coatings, the abrasion resistance is obviously lower after 1000 cycles.

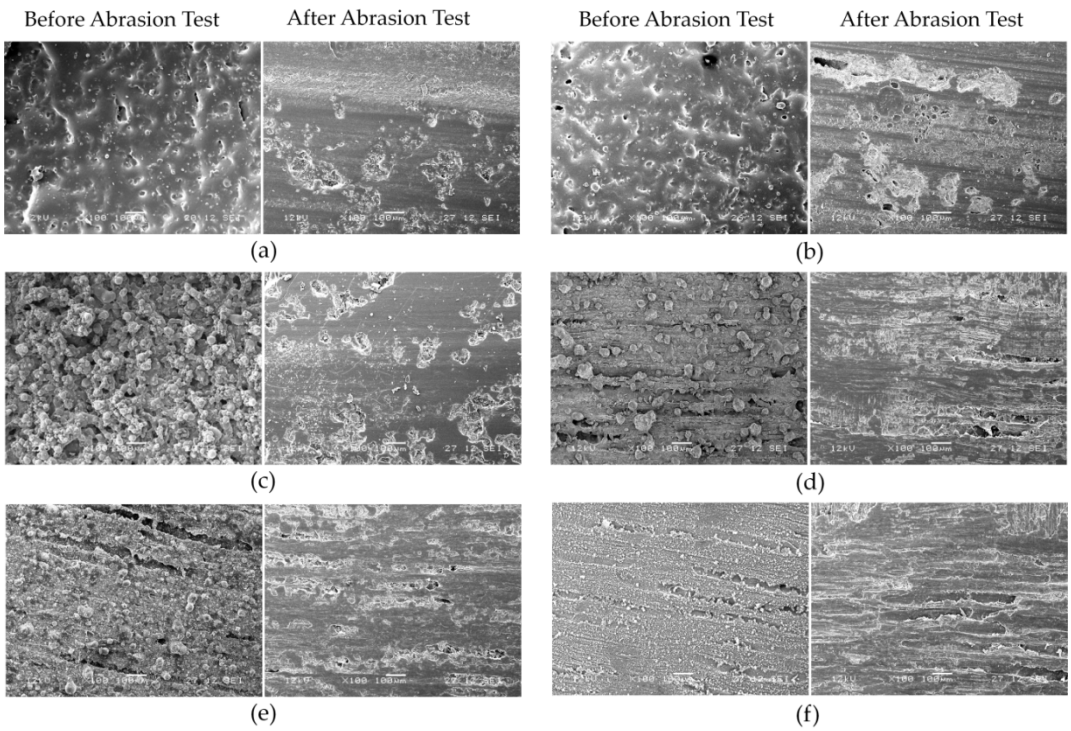

Figure 8. SEM images at magnification of 100× (scale bar 100 µm) of coatings on wood substrates before and after abrasion test. (**a**) polyester thick film; (**b**) polyester thin film; (**c**) polyester/TiO_2 thick film (**d**) polyester/TiO_2 thin film; (**e**) polyester/TiO_2 thin film via (PSP); (**f**) TiO_2 film.

Table 5. Average surface roughness before and after abrasion.

Sample	Roughness before Abrasion *Sa* (μm)	Roughness after Abrasion *Sa* (μm)
Polyester thick film	18.83	10.34
Polyester thin film	21.39	5.08
Polyester/ TiO_2 thick film	40.09	8.50
Polyester/ TiO_2 thin film	8.98	5.26
Polyester/ TiO_2 film via (PSP)	8.06	3.25
TiO_2 film	5.29	3.14

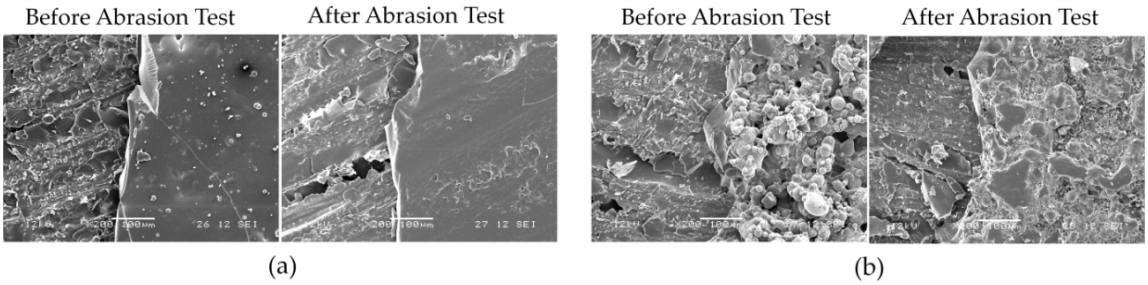

Figure 9. SEM images at magnification of 200x (scale bar 100 μm) of cross-sections before and after abrasion test of: (**a**) polyester thick film; (**b**) polyester/TiO_2 thick film.

Figure 9a,b show the cross-sectional SEM-images of wood surfaces coated with the polyester and polyester/TiO_2 thick films before and after the abrasion test, respectively. Interestingly, it was found after the abrasion test, that under the quasi-spherical polyester/TiO_2 agglomerates layer, there were more molten agglomerates with a great adhesion to the wood substrates.

3.6. Contact Angle Analysis (Water)

The wettability behaviour of the uncoated and coated wood surfaces was investigated by water contact angle (WCA) measurements. The shapes of water droplets on the wood surfaces are shown in Figure 10. The average water contact angle values for the uncoated and coated beech wood surfaces are reported in Table 6. As anticipated, the uncoated wood exhibits hydrophilic behaviour with an average WCA of 45° (Figure 10a). After the coating on hydrophilic wood with polyester, it still exhibits hydrophilic behaviour with an average WCA of 55° (Figure 10b), whereas after coating with TiO_2 from TTIP, and polyester/TiO_2, it shows excellent water repellency; the wood surface transformed from hydrophilic to superhydrophobic, as shown in Figure 10c–e, respectively. Additionally, some of the water droplets rolled on the polyester/TiO_2-coated surfaces, indicating their superhydrophobic behaviour. The polyester/TiO_2 film obtained via the (PSP) method shows hydrophilic behaviour as shown in Figure 10f.

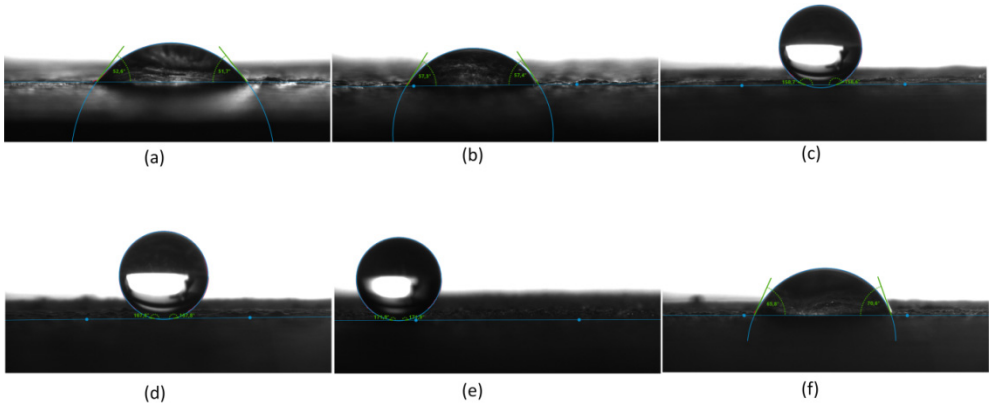

Figure 10. Water contact angle on different surfaces. (**a**) uncoated wood beech; (**b**) polyester thick film; (**c**) TiO_2 film; (**d**) polyester/TiO_2 thick film; (**e**) polyester/TiO_2 thin film; (**f**) polyester/TiO_2 film via (PSP).

Table 6. Average water contact angle values for the beech wood surfaces before and after the abrasion test.

Samples	Contact Angle (°) before Abrasion	Contact Angle (°) after Abrasion
Uncoated wood	45 ± 3	-
Polyester thick film	55 ± 2	73 ± 3
TiO_2 film	>160	45 ± 4
Polyester/TiO_2 thick film	>170	102 ± 2
Polyester/TiO_2 thin film	>170	81 ± 1
Polyester/TiO_2 film via (PSP)	65 ± 4	80 ± 4

The achieved superhydrophobicity of the polyester/TiO_2-coated wood surfaces obtained via the (PSP + LPPS) coating technique method can be attributed to the rough surface with trapped air in the pores of the coated wood [40]. These results could be explained by Wenzel and Cassie-Baxter models. According to the Wenzel model [41], the surface roughness of the substrate should be enlarged to get a high hydrophobicity of surfaces. According to the Cassie-Baxter model [42], air pockets are presumed to be trapped underneath the liquid in rough surface pores in such way that the liquid cannot penetrate into these pores, leading to an enhancement in the hydrophobic behaviour of the surface. The deposition of polyester/TiO_2 coatings on the wood surface via the combination of plasma powder and the liquid precursor coating technique facilitates the formation of high roughness on the wood substrate, as shown from SEM-images. Therefore, it leads to an increasing of the contact angle of water. The hydrophilic behaviour of the wood surfaces covered with a polyester/TiO_2 coating obtained via the (PSP) coating technique can be attributed to their different morphology. The coatings obtained via the (PSP) technique did not completely cover the wood surface, thus hydrophilic behaviour of the surface resulted.

The WCA change of the abraded wood surface was measured after 1000 cycles of abrasion. As shown in Table 6, all of the superhydrophobicity of the coated wood surfaces was destroyed after abrasion. This destruction of the superhydrophobicity can be explained by the loss of the microscale roughness of the abraded wood surface. For example, the roughness of the wood surface coated with thick polyester/TiO_2 coating was smoothed after the abrasion testing, which decreased the WCA of the surface to 102°. From SEM results for samples after abrasion testing, the wood surfaces coated with thin polyester/TiO_2 coatings obtained via both deposition methods got similar structures. As a result, the WCAs on both surfaces were about 80°. The pure TiO_2 coating was almost completely removed from the wood surface after only 100 cycles of abrasion, resulting in the dramatic decrease of the WCA.

4. Conclusions

The SEM results demonstrated that the polyester/TiO_2 films were successfully formed on the wood surfaces by using atmospheric pressure plasma jet (APPJ) in two methods. The morphological differences between TiO_2, polyester, and the polyester/TiO_2 heterostructure were clearly observed using corresponding SEM images. In particular, for samples coated with thin coatings, the wood structure was still clearly visible while the thick coatings completely covered the original wood surface. The results of XPS and the FTIR spectra of the coated and uncoated wood demonstrate that the wood surface was covered with polyester/TiO_2 coatings. After coating of the hydrophilic wood surfaces with TiO_2 from TTIP and polyester/TiO_2 obtained via the combination of plasma powder and the liquid precursor coating technique, the surfaces show excellent water repellency; the wood surfaces were transformed to superhydrophobic. However, the wood surface coated with the polyester/TiO_2 coatings obtained via the (PSP) technique was still hydrophilic. The wood surface after coating with the polyester/TiO_2 composite is more stable with respect to colour change after exposure to UVA radiation than the untreated wood. So, the wood surface was protected from damage under outdoor conditions. The abrasion test results indicated that the polyester-containing films had good abrasion resistance and adhesion to the wood substrates.

Author Contributions: Conceptualization, G.J.; Methodology, G.J.; Validation, G.J., G.O., and W.V.; Investigation, G.J.; Resources, G.O. and W.V.; Writing-Original Draft Preparation, G.J.; Writing-Review and Editing, G.J., G.O. and W.V. All authors have read and agreed to the published version of the manuscript.

Funding: This research was funded by the Lower Saxony Ministry of Science and Culture (MWK). The authors thank the German Research Foundation (DFG) INST 196/11-1 for financial support.

Acknowledgments: The authors further thank Roger Skarsten for proofreading the manuscript.

Conflicts of Interest: The authors declare no conflict of interest.

References

1. Fengel, D.; Wegener, G. *Wood Chemistry, Ultrastructure, Reactions*; Walter de Gruyter: Berlin, Germany, 1984.
2. Feist, W.C.; Hon, D.S. Chemistry of weathering and protection. In *The Chemistry of Solid Wood*; Rowell, R.M., Ed.; American Chemical Society: Washington, DC, USA, 1984; Volume 207, pp. 401–451.
3. Judeinstein, P.; Sanchez, C. Hybrid organic–inorganic materials: A land of multidisciplinarity. *J. Mater. Chem.* **1996**, *6*, 511–525. [CrossRef]
4. Sanchez, C.; Julián, B.; Belleville, P.; Popall, M. Applications of hybrid organic–inorganic nanocomposites. *J. Mater. Chem.* **2005**, *15*, 3559–3592. [CrossRef]
5. Yano, S.; Iwata, K.; Kurita, K. Physical properties and structure of organic–inorganic hybrid materials produced by sol–gel process. *Mater. Sci. Eng. C* **1998**, *6*, 75–90. [CrossRef]
6. Wen, J.; Wilkes, G.L. Organic/Inorganic Hybrid Network Materials by the Sol-Gel Approach. *Chem. Mater.* **1996**, *8*, 1667–1681. [CrossRef]
7. Mir, S.H.; Nagahara, L.A.; Thundat, T.; Mokarian-Tabari, P.; Furukawa, H. Organic-inorganic hybrid functional materials: An integrated platform for applied technologies. *J. Electrochem. Soc.* **2018**, *165*, 3137–3156. [CrossRef]
8. Flores Tandy, L.M.; Perez Bueno, J.J.; Meas Vong, Y. Multifunctional Polymer/Nano-TiO_2 Photochromic Hybrid Coatings as a Barrier for Protection against Corrosion. In *Handbook of Research on Diverse Applications of Nanotechnology in Biomedicine, Chemistry, and Engineering*; United States of America by Engineering Science Reference (an imprint of IGI Global): Hershey, PA, USA, 2014.
9. Altan, M.; Yildirim, H. Mechanical and Antibacterial Properties of Injection Molded PP/TiO_2 Nano-Composites: Effects of Surface Modification. *J. Mater. Sci. Technol.* **2012**, *28*, 686–692. [CrossRef]
10. Segura González, E.A.; Olmos, D.; Lorente, M.Á.; Vélaz, I.; González-Benito, J. Preparation and Characterization of Polymer Composite Materials Based on PLA/TiO_2 for Antibacterial Packaging. *Polymers* **2018**, *10*, 1365. [CrossRef]

11. Kubacka, A.; Fernández-García, M.; Cerrada, M.L.; Fernández-García, M. Titanium Dioxide–Polymer Nanocomposites with Advanced Properties. In *Nano-Antimicrobials: Progress and Prospects*; Springer: Berlin, Germany, 2012; pp. 119–149.
12. Ghaebi Mehmandoust, S.; Alizadeh, R.; Babaluo, A.A. Kinetic study of the poly(vinyl chloride)/titanium dioxide nanocomposites photodegradation under accelerated ultraviolet and visible light exposure. *Polym. Adv. Technol.* **2014**, *25*, 799–808. [CrossRef]
13. Ghanem, A.; Badawy, A.; Ismail, N.; Tian, Z.; Rehim, M.; Rabia, A. Photocatalytic activity of hyperbranched polyester/TiO_2 nanocomposites. *Appl. Catal. Gen.* **2014**, *472*, 191–197. [CrossRef]
14. Koltsakidou, A.; Terzopoulou, Z.; Kyzas, G.Z.; Bikiaris, D.N.; Lambropoulou, D.A. Biobased Poly(ethylene furanoate) Polyester/TiO_2 Supported Nanocomposites as Effective Photocatalysts for Anti-inflammatory/Analgesic Drugs. *Molecules* **2019**, *24*, 564. [CrossRef]
15. Peña, J.; Vallet-Regí, M.; San Román, J. TiO_2-polymer composites for biomedical applications. *J. Biomed. Mater. Res.* **1997**, *35*, 129–134. [CrossRef]
16. Hashimoto, K.; Irie, H.; Fujishima, A. TiO_2 photocatalysis: A historical overview and future prospects. *Jpn. J. Appl. Phys.* **2005**, *44*, 8269–8285. [CrossRef]
17. Linsebigler, A.L.; Lu, G.; Yates, J.T. Photocatalysis on TiO_2 surfaces: Principles, mechanisms, and selected results. *Chem. Rev.* **1995**, *95*, 735–758. [CrossRef]
18. Liu, X.H.; Fu, Y.B. Studies on the structures and optical properties of TiO_2 doped with transition metals. In Proceedings of the 8th Pacific Rim International Congress on Advanced Materials and Processing, Waikoloa, HI, USA, 4–9 August 2013; pp. 295–305.
19. Fanelli, F.; Mastrangelo, A.; Fracassi, F. Aerosol-Assisted Atmospheric Cold Plasma Deposition and Characterization of Superhydrophobic Organic–Inorganic Nanocomposite Thin Films. *Langmuir* **2014**, *30*, 857–865. [CrossRef] [PubMed]
20. Dembele, A.; Rahman, M.; Reid, I.; Twomey, B.; MacElroy, D.; Dowling, D.P. Deposition of Hybrid Organic–Inorganic Composite Coatings Using an Atmospheric Plasma Jet System. *J. Nanosci. Nanotechnol.* **2011**, *11*, 8730–8737. [CrossRef] [PubMed]
21. Buske, C. Environmentally friendly and cost-saving Atmospheric-pressure plasma technology. *Innov. Surf. Technol.* **2009**, *2*, 18–22.
22. Dong, S.; Zhao, Z.; Dauskardt, R.H. Highly transparent bilayer organosilicate multifunctional coatings on plastics deposited by atmospheric plasma deposition with dual organic and inorganic precursors in air. *ACS Appl. Mater. Interf.* **2015**, *7*, 17929–17934. [CrossRef]
23. Pappas, D. Status and potential of atmospheric plasma processing of materials. *J. Vac. Sci. Technol. A Vac. Surf. Films* **2011**, *29*, 020801. [CrossRef]
24. Joshi, S.V.; Sivakumar, G.; Raghuveer, T.; Dusane, R.O. Hybrid plasma-sprayed thermal barrier coatings using powder and solution precursor feedstock. *J. Ther. Spray Technol.* **2014**, *23*, 616–624. [CrossRef]
25. Lohia, A.; Sivakumar, G.; Ramakrishna, M.; Joshi, S.V. Deposition of Nanocomposite Coatings employing a Hybrid APS + SPPS Technique. *J. Therm. Spray Technol.* **2014**, *23*, 1054–1064. [CrossRef]
26. Zhang, W.; Li, G.; Zhang, Q.; Yang, G.; Zhang, G.; Mu, H. Bimodal TBCs with low thermal conductivity deposited by a powder-suspension co-spray process. *J. Mater. Sci. Technol.* **2018**, *34*, 1293–1304. [CrossRef]
27. Jnido, G.; Ohms, G.; Viöl, W. Deposition of TiO_2 Thin Films on Wood Substrate by an Air Atmospheric Pressure Plasma Jet. *Coatings* **2019**, *9*, 441. [CrossRef]
28. Köhler, R.; Sauerbier, P.; Militz, H.; Viöl, W. Atmospheric Pressure Plasma Coating of Wood and MDF with Polyester Powder. *Coatings* **2017**, *7*, 171. [CrossRef]
29. Köhler, R.; Sauerbier, P.; Ohms, G.; Viöl, W.; Militz, H. Wood Protection through Plasma Powder Deposition—An Alternative Coating Process. *Forests* **2019**, *10*, 898. [CrossRef]
30. Wallenhorst, L.; Gurău, L.; Gellerich, A.; Militz, H.; Ohms, G.; Viöl, W. UV-blocking properties of Zn/ZnO coatings on wood deposited by cold plasma spraying at atmospheric pressure. *Appl. Surf. Sci.* **2018**, *434*, 1183–1192. [CrossRef]
31. Fakhouri, H.; Ben Salem, D.; Carton, O.; Pulpytel, J.; Arefi-Khonsari, F. Highly effcient photocatalytic TiO_2 coatings deposited by open air atmospheric pressure plasma jet with aerosolized TTIP precursor. *J. Phys. D Appl. Phys.* **2014**, *47*, 265301. [CrossRef]
32. Mokrzycki, W.S.; Tatol, M. Colour difference ΔE—A survey. *J. Mach. Graph. Vis.* **2011**, *20*, 383–411.

33. Ozen, E.; Yeniocak, M.; Colak, M.; Koca, I. Colourability of wood material with punica granatum and morus nigra extracts. *Bioresources* **2014**, *9*, 2797–2807. [CrossRef]
34. Sun, Q.; Lu, Y.; Zhang, H.; Zhao, H.; Yu, H.; Xu, J.; Fu, Y.; Yang, D.; Liu, Y. Hydrothermal fabrication of rutile TiO_2 submicrospheres on wood surface: An efficient method to prepare UV-protective wood. *Mater. Chem. Phys.* **2012**, *133*, 253–258. [CrossRef]
35. Pavel, P.; Aljaž, V.; Marko, P.; Andrijana, S.; Mohor, M.; Angela, S.; Urban, N.; Boris, O. Structural studies of TiO_2/wood coatings prepared by hydrothermal deposition of rutile particles from $TiCl_4$ aqueous solutions on spruce (Picea Abies) wood. *Appl. Surf. Sci.* **2016**, *372*, 125–138.
36. Santos, L.; Carone, L.P.; Einloft, O.; Ligabue, R.A. Preparation and properties of aromatic polyester/TiO_2 nanocomposites from polyethylene terephthalate. *Mat. Res.* **2016**, *19*, 158–166. [CrossRef]
37. Sirohi, S.; Singh, R.; Jain, N.; Pani, B.; Dutt, K.; Nain, R. Synthesis and characterization of multifunctional ZnO/polyester green composite films. *J. Polym. Res.* **2017**, *24*, 193. [CrossRef]
38. George, G.A. High resolution XPS of organic polymers—The scienta ESCA 300 data base. *Polym. Int.* **1994**, *33*, 439–440. [CrossRef]
39. *Optics, Photonics-Optical Coatings, Part 4: Specific Test Methods*; ISO 9211-4; International Organization for Standardization; ISO: Geneva, Switzerland, 2012.
40. Quéré, D. Wetting and roughness. *Annu. Rev. Mater. Res.* **2008**, *38*, 71–99. [CrossRef]
41. Wenzel, R.N. Surface roughness and contact angle. *J. Phys. Chem.* **1949**, *53*, 1466–1467. [CrossRef]
42. Cassie, A.B.D.; Baxter, S. Wettability of porous surfaces. *Trans. Faraday Soc.* **1944**, *40*, 546–551. [CrossRef]